

# ESI

## Chiral Induced Synthesis of Helical Polypyrrole (PPy) Nano-Structures: A Light-weight and High-Performance Material against Electromagnetic Pollution

Aming Xie,<sup>ab</sup> Fan Wu,<sup>ab\*</sup> Wanchun Jiang,<sup>b</sup> Kun Zhang,<sup>a</sup> Mengxiao Sun,<sup>b</sup> Mingyang Wang<sup>ab</sup>

<sup>a</sup> *School of Mechanical Engineering, Nanjing University of Science & Technology, Nanjing 210094, P. R. China.*

<sup>b</sup> *State Key Laboratory for Disaster Prevention & Mitigation of Explosion & Impact, PLA University of Science and Technology, Nanjing 210007, P. R. China.*

Corresponding authors: [wufanjlg@163.com](mailto:wufanjlg@163.com) (Fan Wu)

Figure S1 shows the X-ray photoelectron spectroscopy (XPS) of LHC-PPy nano-fiber. The N 1s peaks were reasonably decomposed into three Gaussian peaks with 400.86, 399.61 and 397.61 eV, respectively, which was corresponded to positively charged nitrogen atoms ( $\text{NH}^+$ ), secondary amine-like structure (NH), and imine-like structure (C=N) of pyrrole ring (Figure S1a).<sup>1</sup> The C 1s peaks can be resolved into five rational Gaussian peaks at 283.86, 284.81, 285.66, 286.81 and 288.56 eV, which can be

assigned to the structures of N-C=C, C-C=C, C-C-N, C-O, and O-C=O, indicating the existence of carbonyl defects in PPy (Figure S1b).<sup>2-4</sup>

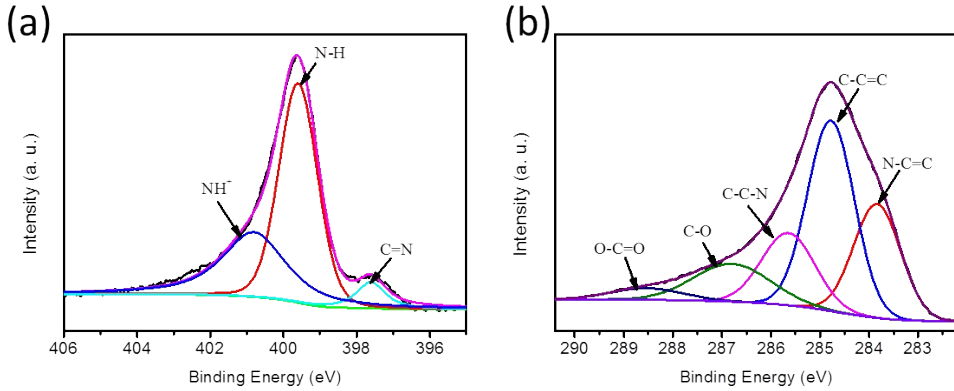


**Figure S1.** XPS core level spectra of N 1s (a) and C 1s (b) of LHC-PPy.

The structure of the LHC-PPy was characterized by Fourier-transform Infrared (FT-IR) detections (Figure S2). The peaks at 1541 cm<sup>-1</sup> is corresponded to the pyrrole ring vibration. The bands at 1454 cm<sup>-1</sup> is assigned to the =CH in-plane vibration of the pyrrole ring and the peaks at 1032 cm<sup>-1</sup> and 960 cm<sup>-1</sup> are owing to the =CH out-of-plane vibration. The bands at 1287 cm<sup>-1</sup> and 1161 cm<sup>-1</sup> corresponds to the stretching vibration of C-N bonds and the C-C stretching, respectively. The band at 1093 cm<sup>-1</sup> is related to in-plane deformation of C-H and N-H bonds of pyrrole ring. It is confirmed that the chemical structure of LHC-PPy is consistent with the PPy particles or PPy aerogel.<sup>5</sup>

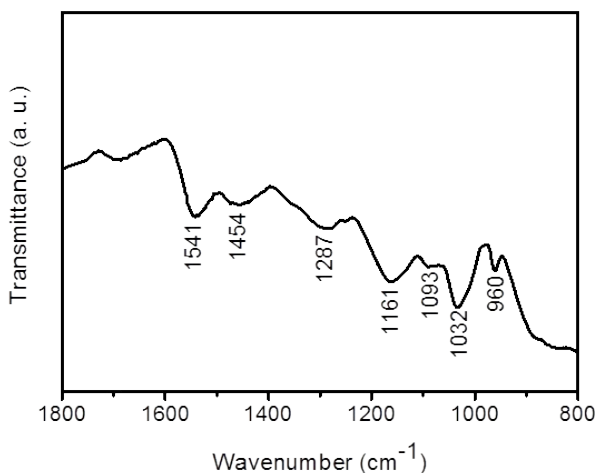


**Figure S2.** FT-IR spectrum of LHC-PPy.

In Figure S3, the Raman spectra of LHC-PPy shows the bands at 925 and 1041 cm<sup>-1</sup> were due to the symmetrical C-H out of plane and in-plane bending, respectively.<sup>5</sup> The peak at 987 cm<sup>-1</sup> was associated with the ring deformation of pyrrole. The C-N stretching aroused the Raman bands at 1335 and 1418 cm<sup>-1</sup>. The C=C stretching shows a strong band at 1570 cm<sup>-1</sup>.

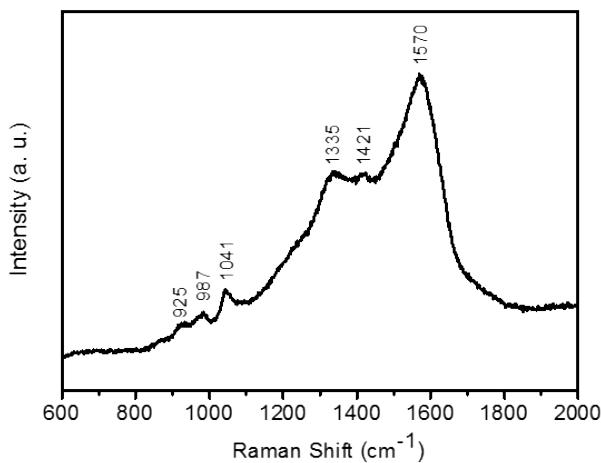


**Figure S3.** Raman spectrum of LHC-PPy.

**Scheme S1** gives the illustration of the mechanisms of EMA and EMI shielding.

**The principle for EMA characterization.** The test process of EMA can be concluded as:

(1) The electromagnetic waves were generated from an emitter. (2) Due to mismatch between the absorber and free space, some electromagnetic waves were reflected and others entered into the absorber vertically. (3) When the electromagnetic waves transmitted in the absorber, some of them were attenuated and transformed to internal energy. (4 and 5) The rest of electromagnetic waves were reflected on the surface of metal backplane, and complicated synergetic enhancement and decrease would be aroused in the reflected electromagnetic waves, due to the resonance at 1/4 wavelength. (6 and 7) Before the reflected electromagnetic waves came back to the free space, partial electromagnetic energy was absorbed in the absorber again.

**The principle for EMI shielding characterization.** The test process of EMI shielding can be concluded as:

(1 and 2) The first two steps are the same as EMA. (3 and 4) When the electromagnetic waves transmitted in the absorber, some of them were attenuated and transformed to internal energy. The others came through the shielding material.

EMA is essentially different from EMI shielding. EMA measures the

difference of energy between the incident and reflected electromagnetic wave while EMI shielding characterizes the difference of energy between the incident and transmitted electromagnetic radiation.

**Scheme S1.** Illustration of the principle for EMA (a) and EMI shielding (b) characterization.

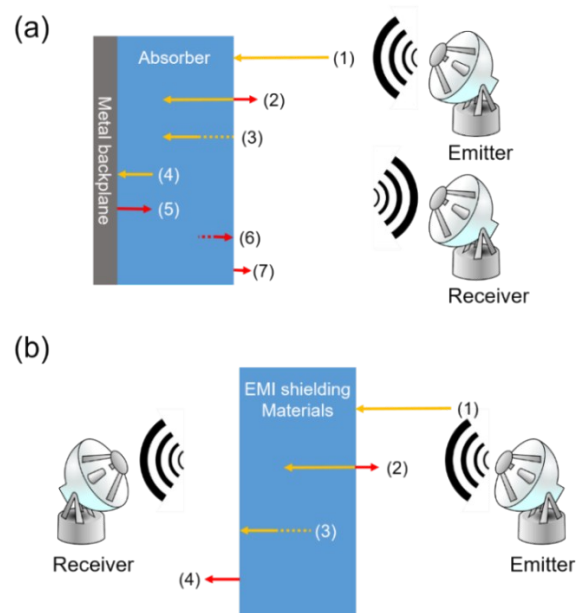


**Table S1. EMA Performance of Typical Materials Reported in This work and Recent Literatures.** (RGO: reduced graphene oxide; PEDOT: poly(3,4-ethylenedioxythiophene); CNCs: Carbon nanocoil; PVDF: polyvinylidene fluoride; PANi: polyaniline; SCI: spherical carbonyl iron; PDA: polydopamine)

Filler	Matrix	Loading ratio (wt. %)	Efficient EMA bandwidth (GHz)	Thickness (mm)	Ref.
DHC-PPy nano-fibers	Wax	7	7.04	2.4	This work
LHC-PPy nano-fibers	Wax	4	6.12	2.4	This work
3D-PPy aerogel	Wax	7	6.20	3	5
3D-PPy/RGO aerogel	Wax	10	6.76	3	6
3D-PPy/PEDOT aerogel	Wax	10	6.28	2.5	7
PANi/Fe <sub>3</sub> O <sub>4</sub> /CNTs	Wax	16	7.00	4	8
Ni/Al <sub>2</sub> O <sub>3</sub> /CNCs	Wax	25	3.60	1.5	9
Porous carbon	Wax	5	4.50	2	10

Fe <sub>3</sub> O <sub>4</sub> /graphene	Wax	10	4.50	1.5	11
Rugby-shaped CoFe <sub>2</sub> O <sub>4</sub>	Wax	50	2.60	2.5	12
Porous Co/C	Wax	40	5.80	2.5	13
SnO <sub>2</sub> foams	Wax	30	5.60	2.0	14
CuS hollow microspheres	Wax	30	3.60	1.8	15
CuS/RGO	Wax	20	4.50	2.5	16
Hollow Fe <sub>3</sub> O <sub>4</sub> -Fe/RGO	Wax	18	6.20	2.0	17
MoS <sub>2</sub> /RGO	Wax	10	5.72	2.0	18
γ-Fe <sub>2</sub> O <sub>3</sub> /RGO	Wax	45	3.00	2.5	19
PEDOT/RGO/Co <sub>3</sub> O <sub>4</sub>	Wax	50	3.10	2.0	20
RGO@hematite	PVDF	5	5.76	2.0	21
RGO/PANi	Wax	10	5.30	3.5	22
RGO/ZnO hollow spheres	Wax	50	3.30	2.2	23

CNTs/RGO	Wax	5	3.50	2.75	24
RGO/MnFe <sub>2</sub> O <sub>4</sub>	Wax	5	4.88	3.0	25
RGO-SCI	Wax	60	4.19	3.0	26
RGO/CNTs	Wax	5	3.30	3.0	27
ZnO@Ni	Wax	60	5.30	1.5	28
RGO/Fe <sub>3</sub> O <sub>4</sub>	Wax	10	5.80	3.0	29
RGO/α-Fe <sub>2</sub> O <sub>3</sub>	Wax	8	6.40	3.0	30
RGO/ZnO	Wax	10	6.40	2.5	31
PPy@PANI	Wax	50	4.70	2.0	32
Ni/SnO <sub>2</sub>	Wax	50	3.80	1.8	33
Hollow PDA@α-MnO <sub>2</sub>	Epoxy	17	3.30	3.0	34
MoS <sub>2</sub> nano-sheets	Wax	60	4.10	2.4	35
ZnO/ZnAl <sub>2</sub> O <sub>4</sub>	Wax	40	4.20	2.86	36

CoO nano-flowers	Epoxy	17	6.00	2.0	37
CF@G@PPy	Wax	20	4.10	2.5	38
Hollow carbon nanosphere	Wax	20	4.8	1.9	39
RGO/ZnO	Wax	20	6.7	2.4	40

**Table S2. EMI SE of composites loaded with LHC and DHC -PPy nano-fibers.**

Fillers	Matrix	Loading ratio (wt. %)	Test frequency range (GHz)	Best EMI SE (dB)	Thickness (mm)
LHC-PPy nano-fibers	Wax	16	2-18	21.82	1
				30.66	2
				43.12	3
				54.72	4
				66.42	5
				78.15	6
DHC-PPy nano-fibers	Wax	16	2-18	17.87	1
				23.18	2
				31.91	3
				40.62	4
				48.64	5
				57.19	6

**Table S3. EMI SE of Typical Materials Reported in Recent Literatures.** (PMMA: polymethylmethacrylate; WPU: water-borne polyurethane; PEI: polyetherimide; PVDF: poly(vinylidenefluoride); PLLA: poly (*L*-lactic acid))

Fillers	Matrix	Loading ratio	Test frequency range (GHz)	Best EMI SE (dB)	Thickness (mm)	Ref.
Porous carbon	Wax	20 wt. %	2-18	50	2.0	10
RGO	PMMA	1.8 vol. %	8-12	<20	4.0	41
RGO	PMMA	4.2 vol. %	8-12	30	3.4	42
RGO	WPU	7.7 wt.%	8.2-12.4	32	2.0	43
RGO	PEI	10 wt. %	8-12	<25	2.3	44
RGO@Fe <sub>3</sub> O <sub>4</sub>	PEI	10 wt. %	8-12	<20	2.5	45
RGO/carbonyl iron	Epoxy	5 wt. %	8-12	<35	2.5	46
CNTs sponge	Epoxy	2 wt. %	8-12	40	2.0	47
RGO	BaTiO <sub>3</sub>	4 wt. %	8.2-12.4	40	1.5	48

CNTs	PVDF	15 wt. %	8-12	57	2.0	49
CNTs	WPU	76 wt. %	8.2-12.4	80	0.8	50
RGO-foam	-	100 wt. %	8-12	25.2	0.3	51
CNTs	PLLA	10 wt. %	8.2-12.4	23	2.5	52
RGO	PU sponge	10 wt. %	8-12	57.7	60	53

## REFERENCES

- (1) Zhong, J.; Gao, S.; Xue, G. and Wang, B. Study on Enhancement Mechanism of Conductivity Induced by Graphene Oxide for Polypyrrole Nanocomposites. *Macromolecules* **2015**, *48*, 1592–1597.
- (2) Ge, H.; Qi, G.; Kang, E. and Neoh, K. G. Study of over Oxidized Polypyrrole Using X-ray Photoelectron Spectroscopy. *Polymer* **1994**, *35*, 504-508.
- (3) Menon, V. P.; Lei, J. and Martin, C. R. Investigation of Molecular and Supermolecular Structure in Template-Synthesized Polypyrrole Tubules and Fibrils. *Chem. Mater.* **1996**, *8*, 2382-2390.
- (4) Zeller, M. V. and Hahn, S. J. The Correlation of Chemical Structure and Electrical Conductivity in Polypyrrole Films by X-ray Photoelectron Spectroscopy. *Surf. Interface Anal.* **1988**, *11*, 327-334.
- (5) Xie, A.; Wu, F.; Sun, M.; Dai, X.; Xu, Z.; Qiu, Y.; Wang, Y. and Wang, M. Self-Assembled Ultralight Three-Dimensional Polypyrrole Aerogel for Effective Electromagnetic Absorption. *Appl. Phys. Lett.* **2015**, *106*, 222902.
- (6) Wu, F.; Xie, A.; Sun, M.; Wang, Y. and Wang, M. Reduced graphene oxide (RGO) modified spongelike polypyrrole (PPy) aerogel for excellent electromagnetic absorption. *J. Mater. Chem. A* **2015**, *3*, 14358-14369.
- (7) Wu, F.; Sun, M.; Jiang, W.; Zhang, K.; Xie, A.; Wang, Y. and Wang,

M. A Self-Assembly Method for the Fabrication of a Three-Dimensional (3D) Polypyrrole (PPy)/Poly(3,4-Ethylenedioxythiophene) (PEDOT) Hybrid Composite with Excellent Absorption Performance Against Electromagnetic Pollution. *J. Mater. Chem. C* **2016**, *4*, 82-88.

(8) Cao, M.; Yang, J.; Song, W.; Zhang, D.; Wen, B.; Jin, H.; Hou, Z. and Yuan, J. Ferroferric Oxide/Multiwalled Carbon Nanotube vs Polyaniline/Ferroferric Oxide/Multiwalled Carbon Nanotube Multiheterostructures for Highly Effective Microwave Absorption. *ACS Appl. Mater. Interfaces* **2012**, *4*, 6948-6955.

(9) Wang, G.; Gao, Z.; Tang, S.; Chen, C.; Duan, F.; Zhao, S.; Lin, S.; Feng, Y.; Zhou, L. and Qin, Y. Microwave Absorption Properties of Carbon Nanocoils Coated with Highly Controlled Magnetic Materials by Atomic Layer Deposition. *ACS Nano* **2012**, *6*, 11009-11017.

(10) Song, W.; Cao, M.; Fan, L.; Lu, M.; Li, Y.; Wang, C. and Ju, H. Highly Ordered Porous Carbon/Wax Composites for Effective Electromagnetic Attenuation and Shielding. *Carbon* **2014**, *77*, 130-142.

(11) Wang, G.; Gao, Z.; Wan, G.; Lin, S.; Yang, P. and Qin, Y. High Densities of Magnetic Nanoparticles Supported on Graphene Fabricated by Atomic Layer Deposition and Their Use as Efficient Synergistic Microwave Absorbers. *Nano Res.* **2014**, *7*, 704-716.

- (12) Zhang, S.; Jiao, Q.; Zhao, Y.; Li, H. and Wu, Q. Preparation of Rugby-Shaped CoFe<sub>2</sub>O<sub>4</sub> Particles and Their Microwave Absorbing Properties. *J. Mater. Chem. A* **2014**, *2*, 18033-18039.
- (13) Lv, Y.; Wang, Y.; Li, H.; Lin, Y.; Jiang, Z.; Xie, Z.; Kuang, Q. and Zheng, L. MOF-Derived Porous Co/C Nanocomposites with Excellent Electromagnetic Wave Absorption Properties. *ACS Appl. Mater. Interfaces* **2015**, *7*, 13604.
- (14) Zhao, B.; Fan, B.; Xu, Y.; Shao, G.; Wang, X.; Zhao, W. and Zhang, R. Preparation of Honeycomb SnO<sub>2</sub> Foams and Configuration-Dependent Microwave Absorption Features. *ACS Appl. Mater. Interfaces* **2015**, *7*, 26217-26225.
- (15) Zhao, B.; Shao, G.; Fan, B.; Zhao, W.; Xie, Y. and Zhang, R. Synthesis of Flower-Like CuS Hollow Microspheres Based on Nanoflakes Self-Assembly and Their Microwave Absorption Properties. *J. Mater. Chem. A* **2015**, *3*, 10345-10352.
- (16) Liu, P.; Huang, Y.; Yan, J.; Yang, Y. and Zhao, Y. Construction of CuS Nanoflakes Vertically Aligned on Magnetically Decorated Graphene and Their Enhanced Microwave Absorption Properties. *ACS Appl. Mater. Interfaces* **2016**, *8*, 5536-5546.
- (17) Qu, B.; Zhu, C.; Li, C.; Zhang, X. and Chen, Y. Coupling Hollow Fe<sub>3</sub>O<sub>4</sub>-Fe Nanoparticles with Graphene Sheets for High-Performance Electromagnetic Wave Absorbing Material. *ACS Appl. Mater.*

*Interfaces* **2016**, *8*, 3730-3735.

- (18) Wang, Y.; Chen, D.; Yin, X.; Xu, P.; Wu, F. and He, M. Hybrid of MoS<sub>2</sub> and Reduced Graphene Oxide: A Lightweight and Broadband Electromagnetic Wave Absorber. *ACS Appl. Mater. Interfaces* **2015**, *7*, 26226-26234.
- (19) Kong, L.; Yin, X.; Zhang, Y.; Yuan, X.; Li, Q.; Ye, F.; Cheng, L. and Zhang, L. Electromagnetic Wave Absorption Properties of Reduced Graphene Oxide Modified by Maghemite Colloidal Nanoparticle Clusters. *J. Phys. Chem. C* **2013**, *117*, 19701-19711.
- (20) Liu, P. Huang, Y. and Sun, X. Excellent Electromagnetic Absorption Properties of Poly(3,4-ethylenedioxythiophene)-Reduced Graphene Oxide-Co<sub>3</sub>O<sub>4</sub> Composites Prepared by a Hydrothermal Method. *ACS Appl. Mater. Interfaces* **2013**, *5*, 12355-12360.
- (21) Chen, D.; Quan, H.; Huang, Z.; Luo, S.; Luo, X.; Deng, F.; Jiang, H. and Zeng, G. Electromagnetic and Microwave Absorbing Properties of RGO@Hematite Core-Shell Nanostructure/PVDF Composites. *Compos. Sci. Technol.* **2014**, *102*, 126-131.
- (22) Chen, X.; Meng, F.; Zhou, Z.; Tian, X.; Shan, L.; Zhu, S.; Xu, X.; Jiang, M.; Wang, L.; Hui, D.; Wang, Y.; Lu, J. and Guo, J. One-Step Synthesis of Graphene/Polyaniline Hybrids by *in situ* Intercalation Polymerization and Their Electromagnetic Properties. *Nanoscale* **2014**, *6*, 8140-8148.

- (23) Han, M.; Yin, X.; Kong, L.; Li, M.; Duan, W.; Zhang, L. and Cheng, L. Graphene-Wrapped Zno Hollow Spheres with Enhanced Electromagnetic Wave Absorption Properties. *J. Mater. Chem. A* **2014**, 2, 16403-16409.
- (24) Kong, L.; Yin, X.; Yuan, X.; Zhang, Y.; Liu, X.; Cheng, L. and Zhang, L. Electromagnetic Wave Absorption Properties of Graphene Modified with Carbon Nanotube/Poly(Dimethyl Siloxane) Composites. *Carbon* **2014**, 73, 185-193.
- (25) Zhang, X.; Wang, G.; Cao, W.; Wei, Y.; Liang, J.; Guo, L. and Cao, M. Enhanced Microwave Absorption Property of Reduced Graphene Oxide (RGO)-MnFe<sub>2</sub>O<sub>4</sub> Nanocomposites and Polyvinylidene Fluoride. *ACS Appl. Mater. Interfaces* **2014**, 6, 7471-7478.
- (26) Zhu, Z.; Sun, X.; Xue, H.; Guo, H.; Fan, X.; Pan, X. and He, J. Graphene-Carbonyl Iron Cross-Linked Composites with Excellent Electromagnetic Wave Absorption Properties. *J. Mater. Chem. C* **2014**, 2, 6582-6591.
- (27) Wang, L.; Huang, Y.; Li, C.; Chen, J. and Sun, X. A Facile One-Pot Method to Synthesize a Three-Dimensional Graphene@Carbon Nanotube Composite as a High-Efficiency Microwave Absorber. *Phys. Chem. Chem. Phys.* **2015**, 17, 2228-2234.
- (28) Wang, G.; Peng, X.; Yu, L.; Wan, G.; Lin, S. and Qin, Y. Enhanced Microwave Absorption of Zno Coated with Ni Nanoparticles Produced

- by Atomic Layer Deposition. *J. Mater. Chem. A* **2015**, *3*, 2734-2740.
- (29) Hu, C.; Mou, Z.; Lu, G.; Chen, N.; Dong, Z.; Hu, M.; Qu, L. 3D Graphene- $\text{Fe}_3\text{O}_4$  Nanocomposites with High-Performance Microwave Absorption. *Phys. Chem. Chem. Phys.* **2013**, *15*, 13038–13043.
- (30) Zhang, H.; Xie, A.; Wang, C.; Wang, H.; Shen, Y.; Tian, X. Novel rGO/ $\alpha$ - $\text{Fe}_2\text{O}_3$  Composite Hydrogel: Synthesis, Characterization and High Performance of Electromagnetic Wave Absorption. *J. Mater. Chem. A* **2013**, *1*, 8547–8552.
- (31) Wu, F.; Xia, Y.; Wang, Y.; Wang, M. Two-Step Reduction of SelfAssembled Three-Dimensional (3D) Reduced Graphene Oxide (RGO)/Zinc Oxide (ZnO) Nanocomposites for Electromagnetic Absorption. *J. Mater. Chem. A* **2014**, *2*, 20307–20315.
- (32) Tian, C.; Du, Y.; Xu, P.; Qiang, R.; Wang, Y.; Ding, D.; Xue, J.; Ma, J. Zhao, H. and Han, X. Constructing Uniform Core-Shell PPy@PANI Composites with Tunable Shell Thickness toward Enhancement in Microwave Absorption. *ACS Appl. Mater. Interfaces* **2015**, *7*, 20090–20099.
- (33) Zhao, B.; Fan, B.; Shao, G.; Zhao, W. and Zhang, R. Facile Synthesis of Novel Heterostructure Based on  $\text{SnO}_2$  Nanorods Grown on Submicron Ni Walnut with Tunable Electromagnetic Wave Absorption Capabilities. *ACS Appl. Mater. Interfaces* **2015**, *7*, 18815–18823.

- (34) She, W.; Bi, H.; Wen, Z.; Liu, Q.; Zhao, X.; Zhang, J. and Che, R. Tunable Microwave Absorption Frequency by Aspect Ratio of Hollow Polydopamine@ $\alpha$ -MnO<sub>2</sub> Microspindles Studied by Electron Holography. *ACS Appl. Mater. Interface* **2016**, *8*, 9782-9789.
- (35) Ning, M.; Lu, M.; Li, J.; Chen, Z.; Dou, Y.; Wang, C.; Rehman, F.; Cao, M. and Jin, H. Two-Dimensional Nanosheets of MoS<sub>2</sub>: A Promising Material with High Dielectric Properties and Microwave Absorption Performances. *Nanoscale*, **2015**, *7*, 15734-15740
- (36) Kong, L.; Yin, X.; Ye, F.; Li, Q.; Zhang, L. and Cheng, L. Electromagnetic Wave Absorption Properties of ZnO-Based Materials Modified with ZnAl<sub>2</sub>O<sub>4</sub> Nanograins. *J. Phys. Chem. C* **2013**, *117*, 2135-2146.
- (37) Li, Y.; Zhang, J.; Liu, Z.; Liu, M.; Lin, H. and Che, R. Morphology-Dominant Microwave Absorption Enhancement and Electron Tomography Characterization of CoO Self-Assembly 3D Nanoflowers. *J. Mater. Chem. C* **2014**, *2*, 5216.
- (38) Wang, C.; Ding, Y.; Yuan, Y.; He, X.; Wu, S.; Hu, S.; Zou, M.; Zhao, W.; Yang, L.; Cao, A. and Li, Y. Graphene aerogel composites derived from recycled cigarette filters for electromagnetic wave absorption. *J. Mater. Chem. C* **2015**, *3*, 11893-11901.
- (39) Zhou, C.; Geng, S.; Xu, X.; Wang, T.; Zhang, L.; Tian, X.; Yang, F.; Yang, H. and Li, Y. Lightweight Hollow Carbon Nanospheres with

Tunable Sizes Towards Enhancement in Microwave Absorption.

*Carbon*, **2016**, *108*, 234-241.

- (40) Feng, W.; Wang, Y.; Chen, J.; Wang, L.; Guo, L.; Ouyang, J.; Jia, D. and Zhou, Y. Reduced Graphene Oxide Decorated with in-situ Growing Zno Nanocrystals: Facile Synthesis and Enhanced Microwave Absorption Properties. *Carbon*, **2016**, *108*, 52-60.
- (41) Zhang, H.; Yan, Q.; Zheng, W.; He, Z. and Yu, Z. Tough Graphene-Polymer Microcellular Foams for Electromagnetic Interference Shielding. *ACS Appl. Mater. Interfaces* **2011**, *3*, 918-924.
- (42) Zhang, H.; Zheng, W.; Yan, Q.; Jiang, Z. and Yu, Z. The Effect of Surface Chemistry of Graphene on Rheological and Electrical Properties of Polymethylmethacrylate Composites. *Carbon* **2012**, *50*, 5117-5125.
- (43) Hsiao, S.; Ma, C. M.; Tien, H.; Liao, W.; Wang, Y.; Li, S. and Huang, Y. Using a Non-Covalent Modification to Prepare a High Electromagnetic Interference Shielding Performance Graphene Nanosheet/Water-Borne Polyurethane Composite. *Carbon* **2013**, *60*, 57-66.
- (44) Ling, J.; Zhai, W.; Feng, W.; Shen, B.; Zhang, J. and Zheng, W. Facile Preparation of Lightweight Microcellular Polyetherimide/Graphene Composite Foams for Electromagnetic Interference Shielding. *ACS Appl. Mater. Interfaces* **2013**, *5*, 2677-

2684.

- (45) Shen, B.; Zhai, W.; Tao, M.; Ling, J. and Zheng, W. Lightweight, Multifunctional Polyetherimide/Graphene@Fe<sub>3</sub>O<sub>4</sub> Composite Foams for Shielding of Electromagnetic Pollution. *ACS Appl. Mater. Interfaces* **2013**, *5*, 11383-11391.
- (46) Chen, Y.; Zhang, H.; Huang, Y.; Jiang, Y.; Zheng, W. and Yu, Z. Magnetic and Electrically Conductive Epoxy/Graphene/Carbonyl Iron Nanocomposites for Efficient Electromagnetic Interference Shielding. *Comp. Sci. Technol.* **2015**, *118*, 178-185.
- (47) Chen, Y.; Zhang, H.; Yang, Y.; Wang, M.; Cao, A. and Yu, Z. High-Performance Epoxy Nanocomposites Reinforced with Three-Dimensional Carbon Nanotube Sponge for Electromagnetic Interference Shielding. *Adv. Mater.* **2016**, *26*, 447-455.
- (48) Qing, Y.; Wen, Q.; Luo, F.; Zhou, W. and Zhu, D. Graphene Nanosheets/BaTiO<sub>3</sub> Ceramics as Highly Efficient Electromagnetic Interference Shielding Materials in the X-Band. *J. Mater. Chem. C* **2016**, *4*, 371-375.
- (49) Wang, H.; Zheng, K.; Zhang, X.; Ding, X.; Zhang, Z.; Bao, C.; Guo, L.; Chen, L. and Tian, X. 3D Network Porous Polymeric Composites with Outstanding Electromagnetic Interference Shielding. *Comp. Sci. Technol.* **2016**, *125*, 22-29.
- (50) Zeng, Z.; Chen, M.; Jin, H.; Li, W.; Xue, X.; Zhou, L.; Pei, Y.;

- Zhang, H. and Zhang, Z. Thin and Flexible Multi-Walled Carbon Nanotube/Waterborne Polyurethane Composites with High-Performance Electromagnetic Interference Shielding. *Carbon* **2016**, *96*, 768-777.
- (51) Shen, B.; Li, Y.; Yi, D.; Zhai, W.; Wei, X. and Zheng, W. Microcellular Graphene Foam for Improved Broadband Electromagnetic Interference Shielding. *Carbon* **2016** *102*, 154-160.
- (52) Kuang, T.; Chang, L.; Chen, F.; Sheng, Y.; Fu, D. and Peng, X. Facile Preparation of Lightweight High-Strength Biodegradable Polymer/Multi-Walled Carbon Nanotubes Nanocomposite Foams for Electromagnetic Interference Shielding. *Carbon* **2016**, *105*, 305-313.
- (53) Shen, B.; Li, Y.; Zhai, W. and Zheng, W. Compressible Graphene-Coated Polymer Foams with Ultralow Density for Adjustable Electromagnetic Interference (EMI) Shielding. *ACS Appl. Mater. Interfaces* **2016**, *8*, 8050-8057.